



This paper is a part of the hereunder thematic dossier published in OGST Journal, Vol. 68, No. 2, pp. 187-396 and available online [here](#)

Cet article fait partie du dossier thématique ci-dessous publié dans la revue OGST, Vol. 68, n°2, pp. 187-396 et téléchargeable [ici](#)

DOSSIER Edited by/Sous la direction de : Jean-Charles de Hemptinne

InMoTher 2012: Industrial Use of Molecular Thermodynamics InMoTher 2012 : Application industrielle de la thermodynamique moléculaire

Oil & Gas Science and Technology – Rev. IFP Energies nouvelles, Vol. 68 (2013), No. 2, pp. 187-396

Copyright © 2013, IFP Energies nouvelles

- 187 > Editorial
- 217 > *Improving the Modeling of Hydrogen Solubility in Heavy Oil Cuts Using an Augmented Grayson Streed (AGS) Approach*
Modélisation améliorée de la solubilité de l'hydrogène dans des coupes lourdes par l'approche de *Grayson Streed Augmenté* (GSA)
R. Torres, J.-C. de Hemptinne and I. Machin
- 235 > *Improving Group Contribution Methods by Distance Weighting*
Amélioration de la méthode de contribution du groupe en pondérant la distance du groupe
A. Zaitseva and V. Alopaeus
- 249 > *Numerical Investigation of an Absorption-Diffusion Cooling Machine Using C_3H_8/C_9H_{20} as Binary Working Fluid*
Étude numérique d'une machine frigorifique à absorption-diffusion utilisant le couple C_3H_8/C_9H_{20}
H. Dardour, P. Cézac, J.-M. Reneaume, M. Bourouis and A. Bellagi
- 255 > *Thermodynamic Properties of 1:1 Salt Aqueous Solutions with the Electrolytic Equation of State*
Propriétés thermophysiques des solutions aqueuses de sels 1:1 avec l'équation d'état de réseau pour électrolytes
A. Zuber, R.F. Checoni, R. Mathew, J.P.L. Santos, F.W. Tavares and M. Castier
- 271 > *Influence of the Periodic Boundary Conditions on the Fluid Structure and on the Thermodynamic Properties Computed from the Molecular Simulations*
Influence des conditions périodiques sur la structure et sur les propriétés thermodynamiques calculées à partir des simulations moléculaires
J. Janeček
- 281 > *Comparison of Predicted pKa Values for Some Amino-Acids, Dipeptides and Tripeptides, Using COSMO-RS, ChemAxon and ACD/Labs Methods*
Comparaison des valeurs de pKa de quelques acides aminés, dipeptides et tripeptides, prédites en utilisant les méthodes COSMO-RS, ChemAxon et ACD/Labs
O. Toure, C.-G. Dussap and A. Lebert
- 299 > *Isotherms of Fluids in Native and Defective Zeolite and Alumino-Phosphate Crystals: Monte-Carlo Simulations with "On-the-Fly" ab initio Electrostatic Potential*
Isothermes d'adsorption de fluides dans des zéolithes silicées et dans des cristaux alumino-phosphatés : simulations de Monte-Carlo utilisant un potentiel électrostatique *ab initio*
X. Rozanska, P. Ungerer, B. Leblanc and M. Yiannourakou
- 309 > *Improving Molecular Simulation Models of Adsorption in Porous Materials: Interdependence between Domains*
Amélioration des modèles d'adsorption dans les milieux poreux par simulation moléculaire : interdépendance entre les domaines
J. Puibasset
- 319 > *Performance Analysis of Compositional and Modified Black-Oil Models For a Gas Lift Process*
Analyse des performances de modèles black-oil pour le procédé d'extraction par injection de gaz
M. Mahmudi and M. Taghi Sadeghi
- 331 > *Compositional Description of Three-Phase Flow Model in a Gas-Lifted Well with High Water-Cut*
Description de la composition des trois phases du modèle de flux dans un puits utilisant la poussée de gaz avec des proportions d'eau élevées
M. Mahmudi and M. Taghi Sadeghi
- 341 > *Energy Equation Derivation of the Oil-Gas Flow in Pipelines*
Dérivation de l'équation d'énergie de l'écoulement huile-gaz dans des pipelines
J.M. Duan, W. Wang, Y. Zhang, L.J. Zheng, H.S. Liu and J. Gong
- 355 > *The Effect of Hydrogen Sulfide Concentration on Gel as Water Shutoff Agent*
Effet de la concentration en sulfure d'hydrogène sur un gel utilisé en tant qu'agent de traitement des venues d'eaux
Q. You, L. Mu, Y. Wang and F. Zhao
- 363 > *Geology and Petroleum Systems of the Offshore Benin Basin (Benin)*
Géologie et système pétrolier du bassin offshore du Benin (Benin)
C. Kaki, G.A.F. d'Almeida, N. Yalo and S. Amelina
- 383 > *Geopressure and Trap Integrity Predictions from 3-D Seismic Data: Case Study of the Greater Ughelli Depobelt, Niger Delta*
Pressions de pores et prévisions de l'intégrité des couvertures à partir de données sismiques 3D : le cas du grand sous-bassin d'Ughelli, Delta du Niger
A.I. Opara, K.M. Onuoha, C. Anowai, N.N. Onu and R.O. Mbach

Improving the Modeling of Hydrogen Solubility in Heavy Oil Cuts Using an Augmented Grayson Streed (AGS) Approach

R. Torres^{1*}, J.-C. de Hemptinne² and I. Machin¹

¹ PDVSA Intevep, Urb. Santa Rosa, Sector El Tambor, Los Teques 1201 - Venezuela

² IFP Energies nouvelles, 1-4 avenue de Bois-Préau, 92852 Rueil-Malmaison Cedex - France
e-mail: roger.torresv@gmail.com – jean-charles.de-hemptinne@ifpen.fr – machini@pdvsa.com

* Corresponding author

Résumé — Modélisation améliorée de la solubilité de l'hydrogène dans des coupes lourdes par l'approche de Grayson Streed Augmenté (GSA) — La méthode de Grayson Streed (GS) [Grayson H.G. and Streed C.W. (1963) *6th World Petroleum Congress*, Frankfurt am Main, Germany, 19-26 June, pp. 169-181] est souvent préconisée dans l'industrie pour calculer la solubilité de l'hydrogène dans des coupes pétrolières. Il se fait cependant que sa précision se dégrade rapidement pour les coupes lourdes. Une amélioration est proposée dans ce travail, basée sur l'ajout d'un terme de Flory dans le calcul du coefficient d'activité.

L'étude de la solubilité de l'hydrogène dans les *n*-alcane du *n*-C₇ au *n*-C₃₆ fait apparaître que la constante de Henry diminue avec la masse molaire. L'analyse de ce comportement suggère la présence d'une déviation entropique à l'idéalité non prise en compte dans le modèle des solutions régulières. L'utilisation d'une correction de Flory permet de garder l'aspect prédictif du modèle. Elle nécessite néanmoins un nouveau calage de certains paramètres de la corrélation d'origine pour l'hydrogène. Le modèle qui résulte se comporte mieux pour les composés lourds et aromatiques.

La qualité du nouveau modèle de Grayson Streed Augmenté (GSA) est évaluée sur des données de solubilité d'hydrogène dans des coupes pétrolières issues de Cai *et al.* [Cai H.Y. *et al.* (2001) *Fuel* 80, 1055-1063] ainsi que Lin *et al.* [Lin H.M. *et al.* (1981) *Ind. Eng. Chem. Process Des. Dev.* 20, 2, 253-256]. L'importance de la caractérisation de ces coupes est mise en avant. Une analyse de sensibilité montre qu'une perturbation du paramètre de solubilité a un effet beaucoup plus important que pour les autres paramètres. Il en résulte qu'un grand soin doit être apporté au calcul de cette grandeur. La prédiction de la solubilité de l'hydrogène dans des fractions pétrolières lourdes et dans des charbons liquéfiés a été améliorée par rapport au modèle de Grayson Streed : une déviation absolue moyenne de 30 % est obtenue pour GSA, à comparer avec 55 % avec la méthode GS, avec les données utilisées dans un domaine de 80-380 °C et 6,3-258,9 bar.

Abstract — Improving the Modeling of Hydrogen Solubility in Heavy Oil Cuts Using an Augmented Grayson Streed (AGS) Approach — The Grayson Streed (GS) method [Grayson H.G. and Streed C.W. (1963) *6th World Petroleum Congress*, Frankfurt am Main, Germany, 19-26 June, pp. 169-181] is often used by the industry for calculating hydrogen solubility in petroleum fluids. However, its accuracy becomes very bad when very heavy fluids are considered. An improvement is proposed in this work, based on a Flory-augmented activity coefficient model.

Hydrogen solubilities in *n*-alkanes from *n*-C₇ up to *n*-C₃₆ have been investigated and a decreasing Henry constant with molecular weight is evidenced. The analysis of the Henry constant behaviour with

molecular weight suggests a simple improvement to the model, using a Flory entropic contribution, thus keeping its predictive character. This improvement led to the necessity of refitting a number of fundamental hydrogen parameters. The resulting model behaves better for heavy components and for aromatics.

The petroleum fractions evaluated with the Augmented Grayson-Streed (AGS) model are taken from Cai et al. [Cai H.Y. et al. (2001) Fuel 80, 1055-1063] and Lin et al. [Lin H.M. et al. (1981) Ind. Eng. Chem. Process Des. Dev. 20, 2, 253-256]. The importance of the petroleum fluid characterization is stressed. A sensitivity analysis has shown that the solubility parameter has a much larger effect than the other parameters: great care must be taken at calculating that property. The predictions of hydrogen solubility in petroleum fractions and in coal liquids were improved compared with the Grayson Streed model, resulting in an Absolute Average Deviation (AAD) of 30% for AGS model compared to 55% for Grayson-Streed model, in the range of 80-380°C and 6.3-258.9 bar.

LIST OF SYMBOLS

A	Derived parameter of the Redlich-Kwong equation
AAD	Average absolute deviation
B	Derived parameter of the Redlich-Kwong equation
D	Relative deviation
Δh_i^{vap}	Molar heat of vaporization of component i
Δh_b^{vap}	Molar heat of vaporization at normal boiling point
Δu_i^{vap}	Molar energy of vaporization of component i
f_i^L	Fugacity of component i in the liquid phase
f_i^{L*}	Fugacity of pure liquid i at T and P of the mixture
f_i^V	Fugacity of component i in the gas phase
G^E	Excess Gibbs energy
H^E	Excess enthalpy
H_i	Henry constant for component i (solute)
K_i	Vaporization equilibrium ratio of component i
k_{ij}	Binary interaction coefficient
N	Total number of data points
P	Pressure
P_{ci}	Critical pressure of component i
P_r	Reduced pressure
P_s^σ	Vapour pressure of the solvent
R	Universal gas constant
S^E	Excess entropy
SG	Specific gravity at 15.5°C
T	Temperature
T_b	Normal boiling temperature
T_{ci}	Critical temperature of component i
T_r	Reduced temperature
v_i	Molar volume of component i
x_i	Mole fraction of component i in the liquid phase
y_i	Mole fraction of component i in the vapour phase
z	Compressibility factor

Greek Letters

γ_i	Activity coefficient of component i at T of the mixture
γ_i^∞	Activity coefficient of component i at infinite dilution

δ_i	Solubility parameter of component i
$\bar{\delta}$	Solubility parameter for the solution
ρ	Density
ρ_T	Density at given temperature T
ϕ_i	Volume fraction of component i in liquid solution
φ_i^{L*}	Fugacity coefficient of pure liquid i at system condition
$\varphi^{(0)}$	Fugacity coefficient of "simple fluids" in liquid state
$\varphi^{(1)}$	Fugacity coefficient correction factor
φ_i^V	Fugacity coefficient of component i in vapour mixture
ω	Acentric factor

INTRODUCTION

As resources of light and conventional crude oils in the world are being depleted, an ever increasing use is made of extra heavy oil and tar sands, which must be converted into clean liquid fuels. The upgrading is achieved through processes such as hydrotreating or hydrocracking. Design and operation of equipments for such processes require the knowledge of the hydrogen solubility in increasingly heavy petroleum mixtures. Reliable estimates of the amount of hydrogen in the hydrocarbon and oil fraction are therefore necessary.

In this work, it is proposed to use the Grayson Streed method to predict hydrogen solubility. The advantage of this method is that it is predictive, as it requires no interaction parameter data. However, for heavy hydrocarbons (greater than C_{15}) the predicted hydrogen solubility may deviate quite bit from experimental values (de Hemptinne *et al.*, 2012). Therefore, it is proposed to add a correction as improvement to this method.

1 LITERATURE REVIEW

Prediction of gas solubility in a liquid solvent is based on the general principles of Vapour-Liquid Equilibrium (VLE) which is formulated through equality of fugacities for each compound between the two phases (Riazi, 2005):

$$f_i^V = f_i^L \quad (1)$$

for all i components at constant T and P , where f_i^V and f_i^L are the fugacities of component i in the gas and liquid phase. These fugacities may be calculated through fugacity coefficients φ_i^V and φ_i^L which leads to the following relation (Riazi, 2005):

$$y_i \varphi_i^V = x_i \varphi_i^L \quad (2)$$

where x_i is the mole fraction of component i in the liquid phase and y_i is the mole fraction of component i in the vapour phase. The fugacity of component i in the liquid phase f_i^L may also be calculated using the deviation from an ideal solution, *i.e.* through activity coefficient, Equation (2) becomes (Riazi, 2005):

$$y_i \varphi_i^V P = x_i \gamma_i f_i^{L*} \quad (3)$$

where f_i^{L*} is the fugacity of pure liquid i at T and P of the mixture. The activity coefficient γ_i depends both on temperature and composition x_i .

The two forms are equivalent but the main difference between Equations (2) and (3) for VLE calculation is in their applications. Equation (2) is particularly useful when both φ_i^V and φ_i^L are calculated from an Equation of State (EoS), in this case, we speak of a homogeneous method. Cubic EoS generally work well for VLE calculation of petroleum fluids at high pressures using Equation (2). This approach is generally preferable, as all thermodynamic relations will be naturally satisfied. This is also the only possible approach for calculations close to a critical point: the only way to satisfy the critical criterion that all phase properties tend to coincide is to use an identical model for all phases (de Hemptinne *et al.*, 2012).

Very often, cubic equations of state are used for calculating φ_i^V and φ_i^L . As a result of the very highly supercritical nature of hydrogen, the EoS must be tuned. Either a modified temperature dependence of the attraction parameter (*e.g.* Twu *et al.*, 1996) or an adequate binary interaction coefficient, that depends on both temperature (*e.g.* Moysan *et al.*, 1983) and the nature of the solvent must then be used. However, the parameters of these models have been adjusted in a restricted temperature range and for a limited number of hydrocarbons for which experimental data were available. As a result, an extrapolation of these interaction coefficients for higher temperatures such as those encountered in hydrotreatment conditions may be questionable (Ferrando and Ungerer, 2007).

More recently, molecular models, such as SAFT (Statistical Association Fluid Theory), have been used with success on this problem (Florusse *et al.*, 2003; Le Thi *et al.*, 2006; Tran *et al.*, 2009). In a similar way as what is conventionally done in molecular simulation techniques (Ferrando and Ungerer, 2007), a group-contribution type approach is proposed. However, these molecular tools, although very promising, require a molecular description of the fluids, which is generally hard to realize for heavy petroleum fractions.

In the case of Equation (3), a different model is used to describe the behaviour of the liquid phase and another to model the vapour phase; in this case, we speak of a heterogeneous approach. This is very useful when the liquid phase non-idealities are significant (de Hemptinne *et al.*, 2012).

The choice of a method for calculating the solubility of hydrogen in heavy oil cuts is guided by two conflicting requirements: the need for accuracy and a search for simplicity.

Shaw (1987) proposed such a correlation adapted to heavy coal liquids and bitumen. The correlation by Shaw provided good predictive results but has to our knowledge not been extensively used in the petroleum refining industry. Instead, the Grayson Streed model is often considered as a "reference" model to simulate hydrogen/hydrocarbon equilibrium. However, it performs poorly for the mixtures involving heavy hydrocarbons (Ferrando and Ungerer, 2007). Hence this model is not the most adequate to predict phase equilibrium data in the operating conditions of hydrotreatments of heavy cuts.

The method of Grayson Streed, available in most process simulators, is a good compromise between accuracy and simplicity. A quick review of the foundations of this method shows that improvements can be introduced for increasing accuracy without losing its simplicity. In this sense, our goal is to propose some variants that can be readily substituted to the original correlation. In the following section a brief review of the fundamentals of the Grayson Streed (Grayson and Streed, 1963) model is presented.

2 THE GRAYSON STREED MODEL (GS)

2.1 How It Works

The Grayson Streed method is based on a heterogeneous, asymmetric approach, in which the distribution coefficient K_i is calculated as follows:

$$K_i = \frac{y_i}{x_i} = \frac{f_i^{L*} \gamma_i}{P \varphi_i^V} = \frac{\varphi_i^{L*} \gamma_i}{\varphi_i^V} \quad (4)$$

where the three factors are calculated using a different model: the pure liquid fugacity coefficient, φ_i^{L*} , is calculated using a specific, corresponding states method. The liquid activity coefficient, γ_i , is calculated using the regular solution model and the vapour phase fugacity coefficient, φ_i^V , is computed from the Redlich Kwong cubic equation of state.

2.1.1 The Pure Liquid Fugacity Coefficient

The fugacity coefficient of pure liquid is calculated with a Curl and Pitzer corresponding state correlation:

$$\log \varphi_i^{L*} = \log \varphi_i^{(0)} + \omega \cdot \log \varphi_i^{(1)} \quad (5)$$

where ω is the acentric factor. The first term on the right hand side represents the fugacity coefficient of “simple fluids”. The second term is a correction accounting for departure of the properties of real fluids from those of “simple fluids”. (Grayson and Streed, 1963)

The quantity $\varphi_i^{(0)}$ depends only on reduced temperature and reduced pressure. It was fitted with the following function by Chao and Seader (1961):

$$\log \varphi_i^{(0)} = A_0 + \frac{A_1}{T_r} + A_2 T_r + A_3 T_r^2 + A_4 T_r^3 + (A_5 + A_6 T_r + A_7 T_r^2) \cdot P_r + (A_8 + A_9 T_r) \cdot P_r^2 - \log P_r \quad (6)$$

where T_r and P_r are the reduced temperature and pressure of the component at hand. Coefficients for Equation (6) were determined by Grayson and Streed (1963) and they are presented in Table 1.

TABLE 1
Coefficients in Equation (6)

Coefficient	Simple fluid	Hydrogen
A_0	2.05135	1.50709
A_1	-2.10899	2.74283
A_2	0.0	-0.02110
A_3	-0.19396	0.00011
A_4	0.02282	0.0
A_5	0.08852	0.008585
A_6	0.0	0.0
A_7	-0.00872	0.0
A_8	-0.00353	0.0
A_9	0.00203	0.0

Source: Grayson and Streed (1963), p. 177.

Special coefficients for Equation (6) are required for hydrogen since the typical application temperatures are far above the critical points of these two compounds. We know that the acentric factor, ω , for this component is not zero but in this work, the assumption of the original work is used and only $\log \varphi^{(0)}$ in Equation (5) is considered for hydrogen (Grayson and Streed, 1963).

The quantity $\varphi_i^{(1)}$ similarly depends only on reduced temperature and reduced pressure and was fitted by Chao and Seader (1961):

$$\log \varphi_i^{(1)} = -4.23893 + 8.65808 \cdot T_r - \frac{1.22060}{T_r} - 3.15224 \cdot T_r^3 - 0.025 \cdot (P_r - 0.6) \quad (7)$$

2.1.2 Activity Coefficient from Regular Solution Theory

The liquid activity coefficient is calculated from the Hildebrand equation, assuming a “regular” liquid solution (no excess volume and no excess entropy). This equation is a liquid phase “molecular” model, proposed by Scatchard (1931) as a result of the work of Hildebrand (1916). It is essentially based on the concepts formulated by Van Laar (Scatchard and Hildebrand, 1934):

$$\ln \gamma_i = \frac{v_i \cdot (\delta_i - \bar{\delta})^2}{R \cdot T} \quad (8)$$

where v_i is the molar volume of component i , δ_i is its solubility parameter and $\bar{\delta}$ is the solubility parameter for the solution, which is calculated as follows (Walas, 1985):

$$\bar{\delta} = \sum_{i=1}^n \phi_i \cdot \delta_i = \sum_{i=1}^n \left(\frac{x_i \cdot v_i}{\sum_{j=1}^n x_j \cdot v_j} \cdot \delta_i \right) \quad (9)$$

The quantity ϕ_i is the volume fraction, *i.e.* the ratio of the molar volume of component i to the weighted molar volume of the mixture. The solubility parameter depends on the temperature but only its value at 25°C is usually taken as the difference between solubility parameters is almost independent of temperature (de Hemptinne *et al.*, 2012). The quantities δ_i and v_i are available in most databases for pure components at 25°C. The parameters used in this work are shown in Table 2.

The solubility parameter can also be calculated from following relation (Riazi, 2005):

$$\delta_i = \sqrt{\frac{\Delta h_i^{vap} - RT}{v_i}} = \sqrt{\frac{\Delta u_i^{vap}}{v_i}} \quad (10)$$

where Δh_i^{vap} is the molar heat of vaporization of component i . As shown in Equation (10), the solubility parameter (δ_i) has a physical meaning. Energy of vaporization is directly related to the energy required to overcome forces between molecules in the liquid phase and molar volume is proportional to the molecular size. Therefore, when two components have similar values of δ their molecular size and forces are very similar yielding an ideal mixture.

The regular solution method is well adapted for non-polar components. It is very powerful in that it only uses physically meaningful pure component parameters. It can therefore be considered as predictive. The following limitations must be borne in mind however:

- it only predicts positive deviations from ideality ($\gamma_i > 1$), *i.e.*, only enthalpy deviation;
- it is not applicable to mixtures of polar components that generally show large deviations from ideality.

2.1.3 Fugacity Coefficient in a Vapour Phase

The Redlich and Kwong equation of state is employed for the calculation of the fugacity coefficient in the vapor mixture. This

coefficient is derived in terms of the compressibility factor Z following the standard procedure (Chao and Seader, 1961):

$$\ln \phi_i^V = (Z-1) \frac{B_i}{B} - \ln(Z-B) + \frac{A}{B} \left[\frac{B_i}{B} - 2 \sqrt{\frac{A_i}{A}} \right] \cdot \ln \left(1 + \frac{B}{Z} \right) \quad (11)$$

$$Z^3 - Z^2 + (A - B - B^2) Z - AB = 0 \quad (12)$$

$$A = \sum \sum (y_i y_j A_{ij}) \quad (13)$$

$$B = \sum (y_i B_i) \quad (14)$$

$$A_{ij} = \sqrt{A_i A_j} \quad (15)$$

$$A_i = 0.42748 \cdot \frac{P_{ri}}{T_{ri}^{2.5}} \quad (16)$$

$$B_i = 0.08664 \cdot \frac{P_{ri}}{T_{ri}} \quad (17)$$

where T_{ri} and P_{ri} are the reduced temperature and reduced pressure of component i .

2.2 Some Results

The Grayson Streed model is evaluated using experimental data on the solubility of hydrogen in pure hydrocarbons. The physical properties of each pure component are summarized in Table 2. The data sources for hydrogen solubility in various pure hydrocarbons are given in Table 3. These data are taken from: Grayson and Streed (1963) for hydrogen, *n*-heptane, *n*-decane and *n*-hexadecane. Yao *et al.* (1977-1978) reported the physical properties for 1-methyl naphthalene, Park *et al.* (1995) for eicosane, octacosane and hexatriacontane. Park *et al.* (1996) for phenanthrene and pyrene. The normal boiling temperatures (T_b) are taken from Riazi (2005), it must be observed at this point that even though the trend of these properties with increasing molecular weight and within a given family, is monotonous, this is not the case for solubility parameters. A maximum is visible for eicosane. This trend is also visible in the data originating from the DIPPR (Design Institute for Physical PRoperties) database.

Since the gas solubility is essentially proportional to the pressure, it is often convenient to use a quantity that considers the ratio of pressure and solubility. The Henry constant of a gas is defined rigorously as follows:

$$H_i = \lim_{x_i \rightarrow 0} \left(\frac{f_i^L}{x_i} \right) \quad (18)$$

where H_i is the Henry constant for component i (solute). It has the unit of pressure. Therefore, H_i is in fact the slope of f_i^L versus x_i at $x_i = 0$. Note that the pressure is necessarily the

TABLE 2
Physical properties of pure components

Fluid name	Formula	MW (g/mol)	$T_b^{(5)}$ (°C)	P_c (Pa)	T_c (K)	ω	v (m ³ /kmol)	δ (J/m ³) ^{0.5}
Hydrogen ⁽¹⁾	H ₂	2.02	-	1 315 524	33.4	0	0.0310	6648
<i>n</i> -Heptane ⁽¹⁾	C ₇ H ₁₆	100.2	98.4	2 735 849	540.2	0.3403	0.1475	15 300
<i>n</i> -Decane ⁽¹⁾	C ₁₀ H ₂₂	142.3	174.2	2 096 013	618.9	0.4869	0.1960	15 793
<i>n</i> -Hexadecane ⁽¹⁾	C ₁₆ H ₃₄	226.4	286.9	1 420 325	723.9	0.7078	0.2942	16 343
Eicosane ⁽²⁾	C ₂₀ H ₄₂	282.6	343.8	1 117 000	770.5	0.8738	0.3598	16 500
Octacosane ⁽²⁾	C ₂₈ H ₅₈	394.7	431.6	826 000	845.4	1.1073	0.5063	16 200
Hexatriacontane ⁽²⁾	C ₃₆ H ₇₄	506.9	497.1	682 000	901.1	1.2847	0.6484	16 200
1-Methylnaphthalene ⁽³⁾	C ₁₁ H ₁₀	142.2	244.7	3 252 533	772.2	0.3020	0.1399	20 046
Phenanthrene ⁽⁴⁾	C ₁₄ H ₁₀	178.2	339.9	3 300 000	873.2	0.5400	0.1580	20 000
Pyrene ⁽⁴⁾	C ₁₆ H ₁₀	202.2	392.8	2 600 000	938.2	0.8300	0.1584	19 670

MW: molecular weight. T_b : normal boiling temperature. P_c : critical pressure. T_c : critical temperature. ω : acentric factor. v : molar volume. δ : solubility parameter.

(1) Source: Grayson and Streed (1963), p. 175.

(2) Source: Park *et al.* (1995), p. 243.

(3) Source: Yao *et al.* (1977-1978), p. 300.

(4) Source: Park *et al.* (1996), p. 72.

(5) The normal boiling temperature (T_b) is taken from Riazi (2005), p. 38.

TABLE 3
Source of experimental data on the solubility of H₂ in pure hydrocarbons

HC type	Fluid name	Nc	Temperature (°C)	Range pressure (bar)	H ₂ solub. (mol%)	Data source
<i>n</i> -Alkane	<i>n</i> -Heptane	7	150-200	3.7-40.5	0.0-5.50	Zernov <i>et al.</i> (1990)
<i>n</i> -Alkane	<i>n</i> -Decane	10	71-310	1.5-255	0.0-50.1	Sebastian <i>et al.</i> (1980) & Park <i>et al.</i> (1995)
<i>n</i> -Alkane	<i>n</i> -Hexadecane	16	189-391	20-254	3.11-51.9	Lin <i>et al.</i> (1980a)
<i>n</i> -Alkane	Eicosane	20	50-300	10-129	1.13-12.9	Park <i>et al.</i> (1995) & Huang <i>et al.</i> (1988)
<i>n</i> -Alkane	Octacosane	28	75-300	10-131	1.49-17.3	Park <i>et al.</i> (1995) & Huang <i>et al.</i> (1988)
<i>n</i> -Alkane	Hexatriacontane	36	100-300	10-168	1.54-22.7	Park <i>et al.</i> (1995) & Huang <i>et al.</i> (1988)
Aromatic	1-Methylnaphthalene	11	189-457	0.25-278	0.00-33.6	Yao <i>et al.</i> (1977-1978) & Lin <i>et al.</i> (1980b)
Aromatic	Phenanthrene	14	110-200	26-252	0.84-8.40	Park <i>et al.</i> (1996) & Malone and Kobayashi (1990)
Aromatic	Pyrene	16	159	52-197	1.59-5.75	Park <i>et al.</i> (1996)
	Overall	7-36	50-457	0.25-278	0.00-51.9	

Nc: carbon number.

HC type: hydrocarbon type.

vapour pressure of the solvent (P_s^σ), because this is the system pressure when the solute concentration reaches zero, as required by the definition. It is considered only as a function of temperature (Riazi, 2005).

Yet, in reality, it is often assumed that the fugacity can be written as a partial pressure (this is particularly true for hydrogen that behaves like an ideal gas up to significant pressures). Using the phase equilibrium relationship, the Henry constant can therefore be estimated from experimental data using:

$$H_i = \frac{y_i P}{x_i} \quad (19)$$

where y_i is the vapour mole fraction of the gas and x_i its mole fraction in the liquid phase. When such experimental values for Henry constant that are plotted as a function of molecular weight at given temperature, a decreasing trend is observed for *n*-alkanes (Fig. 1). Only the first component (*n*-heptane) does not follow the trend. This is probably the result of the fact that the hydrogen solubility range for these data is smaller, indicating that the Henry regime is not fully reached for all data. We may conclude from this observation that the uncertainty on the “experimental” Henry constants is rather large. This is why only the trends will be investigated rather than the actual values. Regressions will be performed on the solubility data rather than on the Henry constants.

Taking into account the definition of f_i^L shown on the right hand side of Equation (3), the Henry constant can be re-written as follow:

$$H_i = \gamma_i^\infty f_i^{L*} \quad (20)$$

where γ_i^∞ is the activity coefficient of component i (here hydrogen) at infinite dilution, *i.e.*, when $x_i \rightarrow 0$ and f_i^{L*} is the

pure component liquid fugacity of the solute i . A relationship between Henry constant (H_i) and the pure liquid fugacity coefficient (φ_i^{L*}) can be derived from Equation (20) and the definition of this fugacity coefficient (φ_i^{L*}):

$$\varphi_i^{L*} = \frac{f_i^{L*}}{P_s^\sigma} = \frac{H_i}{P_s^\sigma \gamma_i^\infty} \quad (21)$$

As mentioned earlier, the pressure is here necessarily the vapour pressure of the solvent (P_s^σ). Subscript i refers to the gaseous component diluted in the solvent, in this work, from here onwards, we will use index 1 to refer to the solute (hydrogen) and index 2 for the solvent. Equation (21) is a useful relationship between Henry’s law and the Grayson Streed model through the pure liquid fugacity coefficient (φ_i^{L*}).

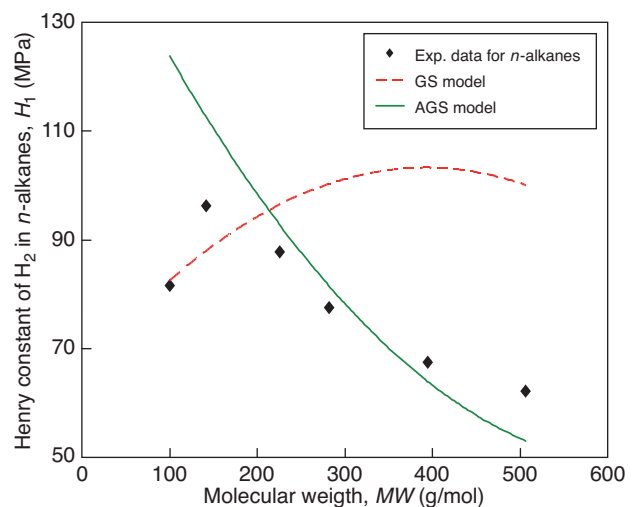


Figure 1

Henry constant of hydrogen in n-alkanes at 423 K.

TABLE 4
Activity coefficient of H₂ at infinite dilution using the Hildebrand model at 423 K

Solvent	Molecular weight, <i>MW</i> (g/mol)	H ₂ fugacity coefficient, φ_1^{L*}	Solv. vap. pressure, P_2^σ (Pa)	H ₂ activity coefficient, γ_1^∞	$\varphi_1^{L*} P_2^\sigma \gamma_1^\infty$ (Pa)
<i>n</i> -Heptane (C ₇ H ₁₆)	100.2	105	374 830	1.934	7.63 × 10 ⁷
<i>n</i> -Decane (C ₁₀ H ₂₂)	142.3	750	52 354	2.089	8.20 × 10 ⁷
<i>n</i> -Hexadecane (C ₁₆ H ₃₄)	226.4	26 626	1 473	2.289	8.98 × 10 ⁷
<i>n</i> -Eicosane (C ₂₀ H ₄₂)	282.6	289 269	135.6	2.352	9.22 × 10 ⁷
<i>n</i> -Octacosane (C ₂₈ H ₅₈)	394.7	28 985 063	1.353	2.234	8.76 × 10 ⁷
<i>n</i> -Hexatriacontane (C ₃₆ H ₇₄)	506.9	2 042 692 112	0.0192	2.234	8.76 × 10 ⁷

On the other hand, rearranging Equation (21) makes it possible to understand how the Grayson Streed model calculates the Henry constant:

$$H_1 = \varphi_1^{L*} P_2^\sigma \gamma_1^\infty \quad (22)$$

The product of $\varphi_1^{L*} P_2^\sigma \gamma_1^\infty$ must follow the same decreasing trend as that of the Henry constant seen in Figure 1. The vapour pressure decreases with increasing hydrocarbon molecular weight, as shown in Table 4, but the hydrogen fugacity coefficient (φ_1^{L*}) increases. As a consequence, the result of $\varphi_1^{L*} P_2^\sigma$ is almost constant, so the trend is almost entirely controlled by the activity coefficient at infinite dilution (γ_1^∞), *i.e.*, γ_1^∞ is the driving element on the Henry constant. The product $\varphi_1^{L*} P_2^\sigma \gamma_1^\infty$ does not follow the correct trend using the Hildebrand model for activity coefficient (dotted line in Fig. 1): it rises continuously until eicosane that has the largest solubility parameter and shows a small decrease beyond.

3 THE FLORY AUGMENTED GS MODEL (AGS)

3.1 Justification

The non-ideal behaviour of a mixture (expressed in terms of excess Gibbs energy) is driven by two major contributions: enthalpic and entropic. This is a direct consequence of the Gibbs energy calculation as a sum of two terms (de Hemptinne *et al.*, 2012):

$$G^E = H^E - TS^E \quad (23)$$

where G^E is the excess Gibbs energy (J); H^E is the excess enthalpy (J) and S^E is the excess entropy (J/K). As a result, the activity coefficient itself can be written as the sum of an enthalpic (or “residual”) and entropic (or “combinatorial”) contribution:

$$\ln \gamma_i = \ln \gamma_i^{res} + \ln \gamma_i^{comb} \quad (24)$$

In the case of regular solutions (Eq. 8), the activity coefficient takes into account only an enthalpic (or “residual”)

contribution as cause of the non-ideal behaviour. However, when the sizes or shapes of molecules are different, an entropic contribution is also expected. In the case of mixtures of large hydrocarbons with hydrogen (very small molecule) the effect of different sizes may be expressed using the Flory model. The final model is simply a combination of the Hildebrand regular solution model (enthalpic) and the Flory model (entropic):

$$\ln \gamma_i = \frac{v_i \cdot (\delta_i - \bar{\delta})^2}{R \cdot T} + \left[\ln \frac{\phi_i}{x_i} + 1 - \frac{\phi_i}{x_i} \right] \quad (25)$$

where ϕ_i again represents the volume fraction of component *i* (see Eq. 9).

The first term on the right hand side of Equation (25) is a positive contribution due to differences in interaction energy; the term between brackets is a negative contribution due to molecular size differences. The combination of these terms makes it possible to represent either positive or negative deviation from Raoult’s law (Robinson and Chao, 1971).

The Flory contribution, as expressed in the second term of Equation (25) is fully predictive in the same way as the first term, which is the Hildebrand contribution. The activity coefficient model that uses the two terms is therefore a very interesting tool for evaluating the trends observed in the non-ideality of mixtures when both entropic and enthalpic effects are present.

In order to improve the required trend for the infinite dilution activity coefficient (Tab. 4), the addition of an entropic contribution will help: this contribution yields a value that is increasingly small as the solvent molar volume increases, as is shown in Table 5.

We can observe that the decreasing trend that is expected for the experimental Henry constant values is much better observed. This is why it is proposed to add a Flory-type entropic contribution as improvement on the calculation of the activity coefficient in the liquid phase.

However, Equation (22) now teaches us that if the value of the infinite dilution activity coefficient has changed, the reference value for the hydrogen liquid phase fugacity, φ_1^{L*} ,

TABLE 5

Flory contribution to activity coefficient of H₂ at infinite dilution in *n*-alkanes at 423 K

Solvent	MW (g/mol)	φ_1^{L*}	P_2^σ (Pa)	γ_1^∞ (Enthalpic)	γ_1^∞ (Entropic)	γ_1^∞ (global)	$\varphi_1^{L*} P_2^\sigma \gamma_1^\infty$ (Pa)
<i>n</i> -Heptane (C ₇ H ₁₆)	100.2	105	374 830	1.934	0.4630	0.895	3.53×10^7
<i>n</i> -Decane (C ₁₀ H ₂₂)	142.3	750	52 354	2.089	0.3670	0.767	3.01×10^7
<i>n</i> -Hexadecane (C ₁₆ H ₃₄)	226.4	26 626	1 473	2.289	0.2578	0.590	2.31×10^7
<i>n</i> -Eicosane (C ₂₀ H ₄₂)	282.6	289 269	135.6	2.352	0.2149	0.505	1.98×10^7
<i>n</i> -Octacosane (C ₂₈ H ₅₈)	394.7	28 985 063	1.353	2.234	0.1565	0.350	1.37×10^7
<i>n</i> -Hexatriacontane (C ₃₆ H ₇₄)	506.9	2 042 692 112	0.0192	2.234	0.1239	0.277	1.09×10^7

Note: φ_1^{L*} is here calculated using the parameters of Table 1.

should also be modified. This is done in this work by modifying the parameters of Equation (6): Table 1 is now replaced by Table 6.

3.2 Parameterization

The reference value for the hydrogen liquid phase fugacity, φ_1^{L*} , is adapted by modifying the parameters that are shown in Table 1. Only parameters A_0 and A_1 are adjusted because according to Equation (6) these parameters affect most strongly the temperature dependence of φ_1^{L*} . In addition, we wanted to modify the original equation as little as possible.

This modification is done by minimization of the sum of square errors between the predicted value by the AGS model ($K_{1,calc}$)_{*i*} and the experimental value ($K_{1,exp}$)_{*i*} on the solubility of hydrogen in pure hydrocarbons. The objective function used to minimize and get the new parameters is as follow:

$$F_{Obj} = \sum_{i=1}^n [\ln(K_{1,calc})_i - \ln(K_{1,exp})_i]^2 \quad (26)$$

where subscript 1 refers to hydrogen and subscript *i* refers to a condition of pressure and temperature (*P*,*T*). The experimental data selected for the parameterization was the same as shown in Table 2. The new coefficients to estimate the liquid fugacity coefficient of hydrogen are shown in Table 6.

3.3 Results

The correct trend of Henry constant with respect to molar mass is observed in Figure 1 (continuous line). Figure 2 presents an overall Absolute Average Deviation (AAD) of Henry constant for each binary system studied. It shows that the AGS model improves the prediction of Henry constant of hydrogen in heavy hydrocarbons, with an overall AAD equal to 11% for *n*-C₁₆₊ and heavy aromatics compounds. In the same way, the prediction of hydrogen solubility in heavy hydrocarbons is improved with the AGS model. A comparative evaluation is shown in Table 7.

TABLE 6

Coefficients for the AGS model in Equation (6) for Hydrogen

Coefficient	Hydrogen
A_0	1.67380
A_1	6.93898
A_2	-0.02110
A_3	0.00011
A_4	0
A_5	0.008585
A_6	0
A_7	0
A_8	0
A_9	0

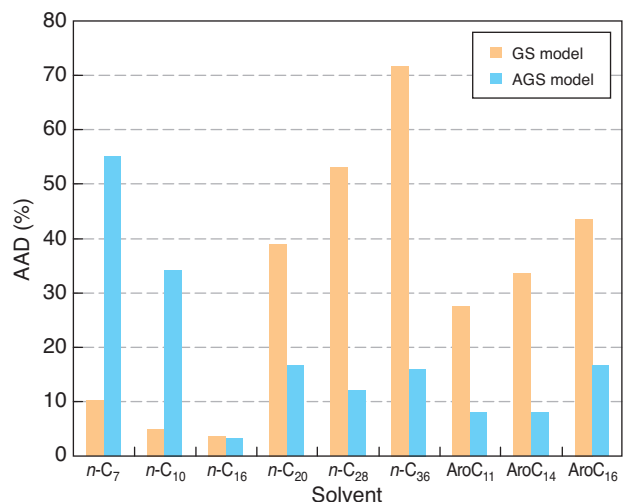


Figure 2

AAD of Henry constant of H₂ in binary mixtures of H₂ + pure hydrocarbon.

TABLE 7

AAD on prediction of H₂ solubility in pure hydrocarbons

System	Number of data	Temperature (°C)	Range pressure (bar)	H ₂ solubility (mol%)	% AAD	
					Grayson Streed	AGS
H ₂ & <i>n</i> -heptane	24	150-200	3.7-40.5	0.0-5.50	8	31
H ₂ & <i>n</i> -decane	47	71-310	1.5-255	0.0-50.1	6	21
H ₂ & <i>n</i> -hexadecane (C ₁₆ H ₃₄)	29	189-391	20-254	3.11-51.9	17	5
H ₂ & eicosane (C ₂₀ H ₄₂)	37	50-300	10-129	1.13-12.9	30	14
H ₂ & octacosane (C ₂₈ H ₅₈)	35	75-300	10-131	1.49-17.3	36	19
H ₂ & hexatriacontane (C ₃₆ H ₇₄)	27	100-300	10-168	1.54-22.7	43	33
H ₂ & methylnaphthalene (C ₁₁ H ₁₀)	40	189-457	0.25-278	0.00-33.6	26	12
H ₂ & phenanthrene (C ₁₄ H ₁₀)	37	110-200	26-252	0.84-8.40	57	12
H ₂ & pyrene (C ₁₆ H ₁₀)	6	159	52-197	1.59-5.75	86	32
Overall	282	50-457	0.25-278	0.00-51.9	29	18

Considering heavy *n*-alkanes (*n*-C₁₆₊) and heavy aromatic compounds, the AAD for the AGS model is 16% vs 36% for the original GS model, indicating a 56% improvement, in the range of 50-457°C and 0.25-278 bar.

The deviations for the low molecular weight solvents are increased: the quality of the regular GS method for these systems was already very good according to the available data. Yet, our focus was to improve the model for the heavy hydrocarbons, which is clearly a success. As a matter of fact, an improvement is visible for all aromatic solvents which were not included in the regression.

Figures 3 and 4 show a comparison between prediction solubility hydrogen with the AGS and the conventional GS models. The improvements with AGS are well visible.

4 APPLICATION TO PETROLEUM CUTS

The AGS model is evaluated on petroleum fractions: two Canadian heavy oils Light Virgin Gas Oil (LVGO) and Heavy Virgin Gas Oil (HVGO) which are typical feed stock for hydroprocessing, a Chinese Heavy Oil (GuDao Atmospheric Residuum, GDAR) and Athabasca Bitumen Vacuum Bottoms (ABVB). Relevant physical properties for these materials are given in Table 8. The normal boiling temperature is estimated from the vapour pressure curves shown by Cai *et al.* (2001). Note that these are in fact bubble temperatures of complex mixtures: they are not average boiling temperatures for the entire cut. Nevertheless, they provide an interesting value which is measured rather than calculated.

4.1 Petroleum Cut Characterization

A pseudo-component method based on the assumption that the petroleum fraction is a single, molecularly homogeneous pseudo-component is used in order to estimate the

characteristic properties (P_c , T_c , ω , ν and δ) of the petroleum fractions.

In this approach, the liquid phase is considered to be a mixture only of two components: the solute (dissolved gas, *i.e.*, hydrogen) and the solvent (petroleum fraction), which are denoted again as components 1 and 2, respectively.

It is known that many methods exist for determining these characteristic properties, as discussed for example by Riazi (2005). Each method yields potentially different characteristic parameters and therefore a more or less different end result. It would be a very extensive job to evaluate all methods for each characteristic property individually. Instead, we first propose a sensitivity analysis. This will allow us, in a second step, to focus our attention on the property which has the largest effect.

TABLE 8

Characterization of petroleum fractions

Property	Unit	LVGO	HVGO	GDAR	ABVB
C	wt%	85.0	84.4	85.4	84.3
H	wt%	13.2	10.8	11.4	10.9
N	wt%	0.4	1.5	0.8	0.8
S	wt%	1.3	3.8	2.5	3.5
Density, ρ at 20°C	g/cm ³	0.892	0.973	0.922	1.05
Distillation range	°C	184-454	274-595	350+	525+
Normal boiling temperature	°C	239.3	340.0	267.5	387.4
Mean molar mass	g/mol	250	350	1 678	1 700
Aromatic carbon	%	15.9	25.4	36.5	35.0
Inorganic solids	ppm	~20	~20		
H/C ratio	mol/mol	1.74	1.52	1.60	1.54

Source: Cai *et al.* (2001), p. 1509.

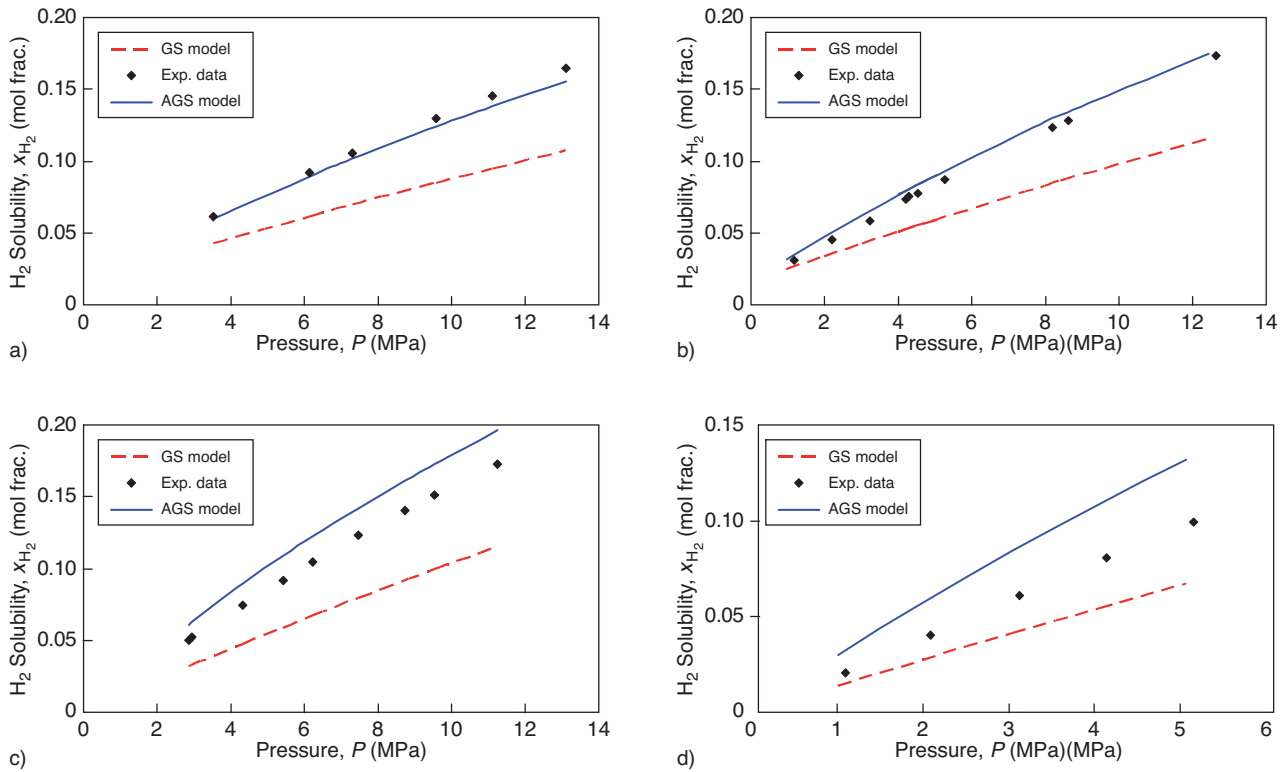


Figure 3

Solubility of hydrogen in octacosane at different temperatures. a) 348 K, b) 373 K, c) 423 K, d) 473 K.

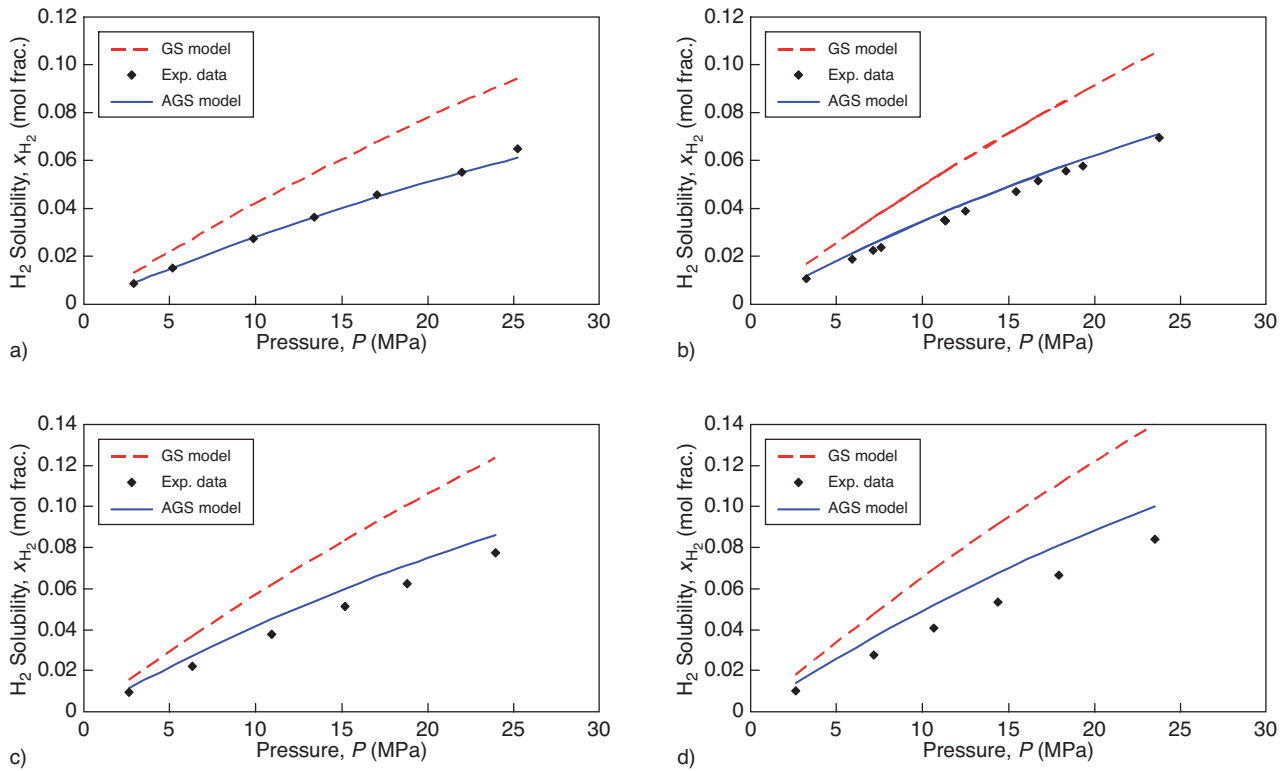


Figure 4

Solubility of hydrogen in phenanthrene at different temperatures. a) 398 K, b) 423 K, c) 448 K, d) 473 K.

4.2 Sensitivity Analysis

This analysis is performed using a base case, in this case H₂ in HVGO and testing the effect of a 10% perturbation on each parameter on turn: solubility parameter (δ), critical pressure (P_c), critical temperature (T_c), acentric factor (ω), molar volume (v) and molecular weight (MW) of the solvent.

The characterization methods used for the sensitivity analysis are listed in Table 9 and a brief description of these methods is given in Appendix A, except for the solubility parameter which is detailed below.

An average on the relative deviation in the calculated hydrogen solubility is computed over all pressure and temperature conditions given by Cai *et al.* (2001).

Table 10 shows the relative deviation on the prediction of hydrogen solubility as response of the perturbation in the parameters. This table shows that the solvent solubility parameter (δ), molar volume (v) and molecular weight (MW), are the most sensitive parameters to estimate the solubility of hydrogen in petroleum fractions. Critical temperature (T_c) has also a non-negligible effect on the hydrogen solubility.

TABLE 9

Method to calculate physical properties of heavy oils

Property	Method	Source
Critical pressure P_c	API	Riazi (2005)
Critical temperature T_c	API	Riazi (2005)
Acentric factor ω	Korsten	Riazi (2005)
Molar volume at 25°C v	Density and molecular weight	Riazi (2005)
Solubility parameter δ	Definition	Equation (10)

TABLE 10

Relative deviation of H₂ solubility due to parameters perturbation

Property	Perturbation	
	10%	-10%
Solubility parameter at 25°C δ_2	-23%	+24%
Molar volume at 25°C V	+8.0%	-8.1%
Molecular weight MW	+6.8%	-7.0%
Critical temperature T_c	+1.5%	-6.1%
Acentric factor ω	+0.2%	-0.2%
Critical pressure P_c	-0.2%	+0.2%

4.3 Evaluation of the Characterization Methods for Petroleum Cuts

Looking at Table 8, it is visible that the lightest cut investigated is LVGO and the heaviest ABVB. Regarding the two other cuts (HVGO and GDAR), the data seem contradictory: density and normal boiling temperature of GDAR are lower,

but molar mass is significantly higher than that of HVGO. The aromatic carbon content is larger, yet the larger H/C ratio indicates it should be lower.

Yet, the resulting properties in Table 11 seem to indicate that ABVB is the heaviest (from the large T_c and acentric factor), while GDAR is slightly heavier than LVGO. This can be readily explained by noting that the characterization method uses density and normal boiling point as input, rather than molar mass. Note that the solubility parameters according to method 1 (Eq. 10) are much too low compared to what is expected from hydrocarbons as shown in Table 3.

As a result of the sensitivity analysis, it appears that the solubility parameter is clearly the most important parameter. This is why three different methods have been tested for calculating this parameter, as shown below the horizontal line of Table 11.

TABLE 11

Physical properties calculated for petroleum fractions

Property	Unit	LVGO	HVGO	GDAR	ABVB
Critical pressure P_c	MPa	2.40	2.50	2.62	3.12
Critical temperature T_c	K	723.9	806.8	741.2	852.4
Acentric factor ω		0.431	0.916	0.644	1.234
Molar volume at 25°C v	m ³ /kmol	0.281	0.361	1.826	1.622
Solubility parameter ¹ at 25°C δ	(J/m ³) ^{0.5}	14 211	16 808	6 284	9 229
Correction factor ² α		0.638	0.777	2.622	2.653
Solubility parameter ³ at 25°C δ	(J/m ³) ^{0.5}	16 452	16 752	17 467	17 470

¹ Calculated by definition (Eq. 10, 27, 28), using Riedel and Watson method for ΔH^{vap} .

² α correction factor modifies the solubility parameter of hydrogen (δ_{H_2}) as follow: $\delta_{H_2, corrected} = \alpha \cdot \delta_{H_2}$. Riazi and Roomi (2007).

³ Calculated by SCN method (Eq. 31), taken from Riazi and Vera (2005).

4.3.1 Solubility Parameter using the Definition

The definition of the solubility parameter is given by Equation (10). It is a function of enthalpy of vaporization at 25°C, which can be calculated in two steps: calculation at the normal boiling point, Δh_b^{vap} and subsequent correction to 25°C. One of most successful correlations for prediction of Δh_b^{vap} was proposed by Riedel (Smith *et al.*, 1996):

$$\frac{\Delta h_b^{vap}}{RT_b} = 1.093 \left(\frac{\ln P_c - 1.013}{0.93 - T_{br}} \right) \quad (27)$$

where R is the universal gas constant and P_c is the critical pressure in bar. The unit of Δh_b^{vap} depends on the unit of R and T_c . Once Δh_b^{vap} is determined, the Watson relation can be used to calculate Δh^{vap} at the desired temperature (T) (Smith *et al.*, 1996):

$$\frac{\Delta h^{vap}}{\Delta h_b^{vap}} = \left(\frac{1 - T_r}{1 - T_{br}} \right)^{0.38} \quad (28)$$

4.3.2 Riazi Correction

We have seen that the activity coefficient in fact depends on the difference between solubility parameters (Eq. 25). Riazi and Roomi (2007) suggest to modify the gas solubility coefficient instead of that of the solvent. They state that the solubility parameter of the gas in a fictitious liquid phase (δ_1) will depend on the molecular weight of this phase. This correction factor is introduced as:

$$\delta_1 = \alpha \delta_{1(GS)} \quad (29)$$

where δ_1 is the corrected solubility parameter for hydrogen, α is the correction factor and $\delta_{1(GS)}$ is the solubility parameter reported by Grayson and Streed (1963). The correction factor depends on the type of gas and solvent (*i.e.*, a petroleum fraction or a coal liquid) but is independent of temperature. For paraffin rich petroleum fractions following relationship is proposed by Riazi and Roomi (2007):

$$\alpha = 0.29 + 0.00139MW \quad (30)$$

This relationship has been developed for paraffinic crudes only because of the lack of sufficient data on naphthenic or aromatic crudes (Riazi and Roomi, 2007).

The petroleum fractions investigated in this work have a relatively low aromatic content (<37%) making it possible to use this correlation.

The solubility parameter of the solvent (δ_2) in this case is calculated using the definition (Eq. 10).

4.3.3 Single Carbon Number (SCN) Approach

The third correlation is based on Riazi and Al-Sahhaf (1996), where following relation is proposed to calculate δ_2 from the molecular weight of the liquid fraction:

$$\delta_2 = 17.5913 - \exp(3.0076 - 0.549097MW^{0.3}) \quad (31)$$

where δ_2 is expressed in $(\text{J}/\text{cm}^3)^{0.5}$. This correlation can be used within the molecular weight range of 80-700 ($\sim C_6-C_{50}$). This value of δ_2 is based on estimated values for properties of Single Carbon Number (SCN) groups (Riazi and Vera, 2005).

Table 11 shows the results of the physical properties including the three options for solubility parameter calculation. It is clear that the solubility parameter value is very different for the three calculation modes. The results obtained from the SCN (Single Carbon Number) method are most reasonable, since the values of the solubility parameter as largest for the heaviest cut, ABVB.

The calculations from the definition are least reasonable because the values found are very small compared to those of hydrocarbons of similar molecular weight (see for example Tab. 3).

4.4 Application to Coal Liquids

Additionally, AGS model is evaluated in two narrow boiling distillate cuts from the Exxon Donor Solvent (EDS) and three narrow boiling distillate cuts from the Solvent Refined Coal II (SRC-II) process. Relevant physical properties for these materials are given in Table 12.

TABLE 12
Characterization of coal liquids

Property	Unit	CLPP A5	CLPP A5	SRC-II	SRC-II	SRC-II
		204-232°C	260-315°C	No. 5	No. 9	No. 12
s.g. at 15°C		0.9320	0.9844	0.9826	1.0306	1.0910
Distillation curve	(°C)					
5%	%	191.1	251.9	233.3	302.2	358.9
10%		197.9	258.7	235.6	303.3	360.0
30%		204.3	272.9	243.3	307.8	362.2
50%	ppm	209.7	285.3	251.1	314.4	363.3
70%	mol/mol	219.3	295.2	261.1	322.2	367.8
90%		230.4	313.2	280.0	336.7	382.2
95%		233.9	319.7	292.2	348.9	392.2
Mean molar mass	g/mol	154.34	182.30	182	212	252
Total aromatics	wt%	71.78	73.09			

TABLE 13
Physical properties calculated for coal liquids

Property	Unit	CLPP A5	CLPP A5	SRC-II	SRC-II	SRC-II	
		204-232°C	260-315°C	No. 5	No. 9	No. 12	
Critical pressure	P_c	MPa	2.94	2.50	2.86	2.56	2.54
Critical temperature	T_c	K	710.8	794.1	758.9	831.7	897.8
Acentric factor	ω		0.364	0.448	0.390	0.455	0.486
Molar volume at 25°C	v	m ³ /kmol	0.167	0.186	0.186	0.207	0.232
Solubility parameter ¹ at 25°C	δ	(J/m ³) ^{0.5}	15 913	16 114	16 112	16 283	16 460

TABLE 14
AAD on prediction of H₂ Solubility in petroleum fraction

Petroleum fraction	No. of data	Temp. (°C)	Range pressure (bar)	H ₂ solub. (mol%)	δ_2 by definition		α factor on δ_1		SCN approach	
					GS	AGS	GS	AGS	GS	AGS
LVGO	38	80-380	11.7-122.7	1.9-23.7	29%	45%	13%	13%	11%	14%
HVGO	43	80-380	6.3-118.8	0.7-42.3	19%	30%	35%	15%	18%	31%
GDAR	33	80-380	6.7-106.0	5.1-60.3	51%	156%	82%	15%	80%	14%
ABVB	29	130-380	7.3-121.2	2.6-70.0	42%	166%	64%	64%	74%	24%
CLPP(204-232°C)	9	190-270	49.6-258.9	0.04-0.22					76%	34%
CLPP(260-315°C)	8	190-270	50.0-254.4	0.03-0.19					96%	62%
SRC-II No. 5	8	190-270	50.7-254.0	0.04-0.20					82%	50%
SRC-II No. 9	8	190-270	48.4-253.0	0.03-0.19					95%	74%
SRC-II No. 12	5	270	51.7-252.7	0.04-0.16					119%	117%
Overall	181	80-380	6.3-258.9	0.03-70.0	35%	73%	48%	23%	55%	30%

GS: Grayson Streed model.

AGS: Augmented Grayson Streed model.

The results of physical properties calculated for the coal liquids are shown in Table 13, in this case the solubility parameter was calculated by SCN method, according to Equation (32).

4.5 Calculation Results and Discussion

Both the GS and AGS models have been run with these three different input data for petroleum fractions and Table 14 shows a summary of the calculations of hydrogen solubility in petroleum fractions, as well as hydrogen solubility in coal liquids. As can be seen, the hydrogen solubility prediction in petroleum fractions is very sensitive to the values of the physical properties. However, the best predictions are obtained with the SCN solubility parameter approach. Except when using the solubility parameter calculated “from the definition”, the predictions of hydrogen solubility are improved compared with the GS model.

For the SCN prediction method, which we recommend here, the Absolute Average Deviation (AAD) is 30% for AGS vs 55% the GS model, including the hydrogen solubility in coal liquids.

Figure 5 shows the prediction of hydrogen solubility in petroleum cuts at given temperatures and Figure 6 shows the Henry constant as a function of temperature predicted by GS and AGS for the petroleum fractions, using the SCN approach to the solubility parameter.

Henry constants predicted by the AGS model are significantly improved compared with the regular GS model. The improvement is most visible for the heavier component. Only for HVGO, could we observe a slight decrease in the quality of the solubility predictions. It is clear that this quality not only depends on the model but also on the values of the characteristic parameters of the petroleum fractions. As discussed above, we may have doubts about the coherence between molar volume and molar mass of this cut.

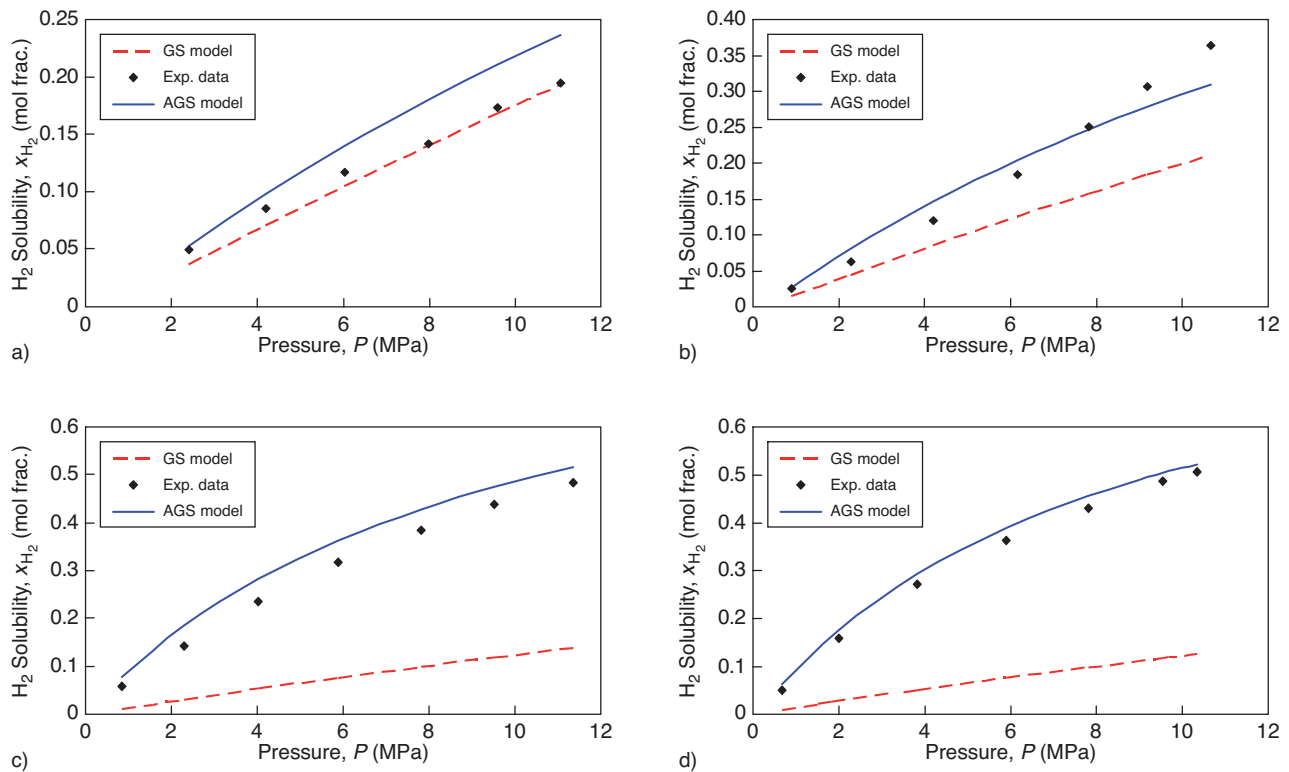


Figure 5

Solubility of hydrogen on heavy petroleum cuts. a) in LVGO at 603 K, b) in HVGO at 653 K, c) in ABVB at 523 K, d) in GDAR at 523 K.

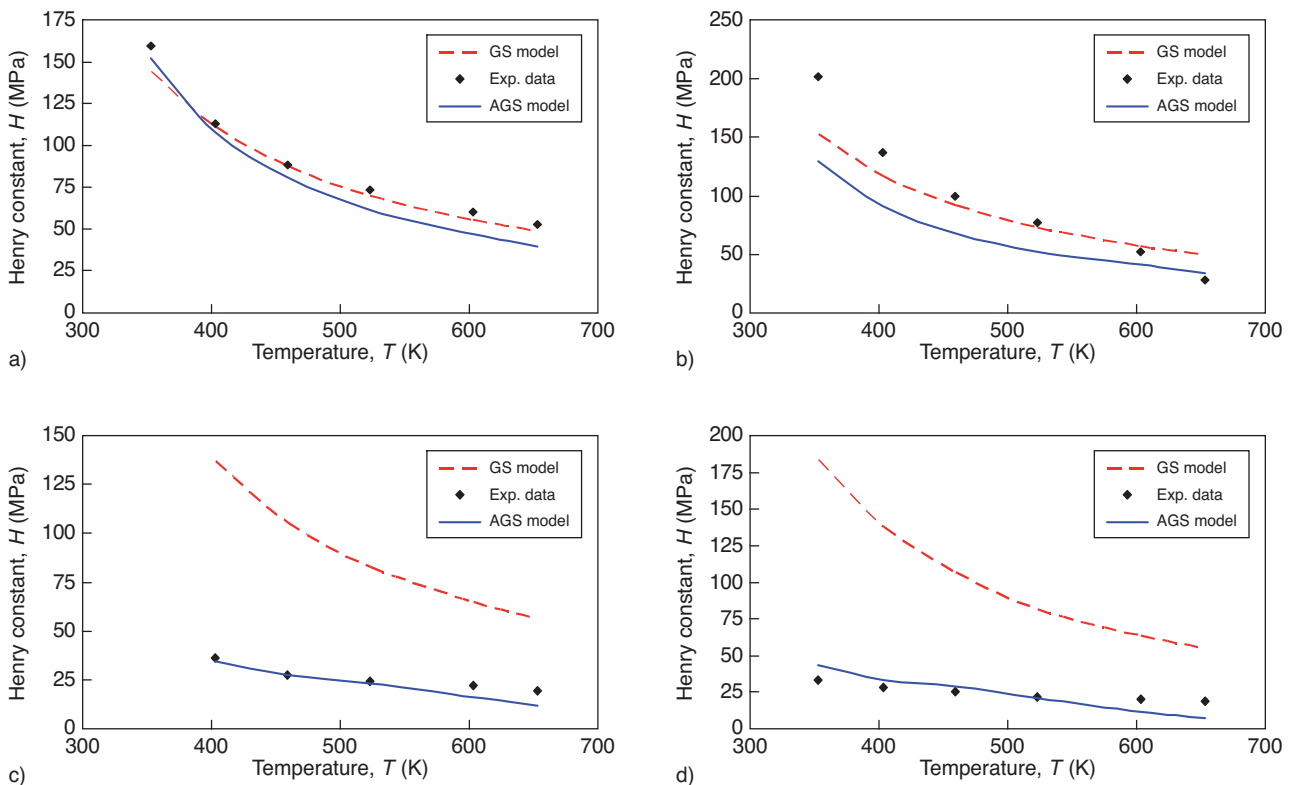


Figure 6

Henry constant of hydrogen in heavy petroleum cuts. a) in LVGO, b) in HVGO, c) in ABVB, d) in GDAR.

In summary, AGS is capable of predicting solubility of hydrogen in various petroleum cuts. However, the main advantage of this method is that in addition to simplicity and availability of input parameters it does not need binary interaction parameters: the approach using the solubility parameter is purely predictive.

CONCLUSION

The Grayson Streed model underestimates the solubility of hydrogen in heavy pure *n*-alkanes and overestimates the solubility of hydrogen in pure aromatic compounds.

In order to improve this behaviour, a simple methodology has been proposed, leading to a new model that reflects more correctly the effect of the entropic contribution when small gas molecules are dissolved in a heavy hydrocarbon solvent. This model, called "Augmented Grayson Street" is based on the addition of an entropic Flory term in the activity coefficient calculation.

New reference values for the hydrogen liquid phase fugacity coefficient, φ_1^{L*} , have been obtained as a result of a change in the infinite dilution activity coefficients for the AGS model.

The AGS model improves the predictions for solubility of hydrogen in heavy *n*-alkanes components (C_{16+}) and also improves the solubility predictions in aromatics. Although a degradation is observed for low molecular weight alkane solvents, the overall AAD for AGS model is 16% vs 36% for GS model, indicating a 56% improvement, in the range of 50–457°C and 0.25–278 bar.

The main difficulty to use the model for hydrogen solubility calculations in petroleum fractions is to find adequate methods to estimate the physical properties of pseudo-component. The model is most sensitive to a correct representation of the solubility parameter for which several prediction methods have been tried. The SCN method (Riazi and Vera, 2005) was found best.

The predictions of hydrogen solubility in petroleum fractions and in coal liquids were improved compared with the Grayson Streed model, with AAD = 30% for AGS model compared to 55% for Grayson Streed model, in the range of 80–380°C and 6.3–258.9 bar.

It should be stressed that other approaches, based on homogeneous equation of state models, may lead to more accurate results. The goal of the analysis proposed in this work is to suggest that for heavy components the sole Hildebrand activity coefficient model is not sufficient.

ACKNOWLEDGMENTS

This work was performed as a master thesis in collaboration between IFP-School and PDVSA. Special thanks to Daniel Dumas who is responsible for this collaboration.

REFERENCES

- Cai H.Y., Shaw J.M., Chung K.H. (2001) Hydrogen solubility measurements in heavy oil and bitumen cuts, *Fuel* **80**, 1055–1063.
- Chao K.C., Seader J.D. (1961) A general correlation of vapor-liquid equilibria in hydrocarbon mixtures, *AIChE J.* **7**, 4, 598–605.
- de Hemptinne J.C., Ledanois J.M., Mougin P., Barreau A. (2012) *Select Thermodynamic Models for Process Simulation*, Editions Technip, Paris.
- Ferrando N., Ungerer P. (2007) Hydrogen/hydrocarbon phase equilibrium modeling with a cubic equation of state and a Monte Carlo method, *Fluid Phase Equilib.* **254**, 1–2, 211–223.
- Florusse L.J., Peters C.J., Pàmies J.C., Vega L.F., Meijer H. (2003) Solubility of hydrogen in heavy *n*-alkanes: Experiments and SAFT modelling, *AIChE J.* **49**, 12, 3260–3269.
- Grayson H.G., Streed C.W. (1963) Vapor-liquid equilibria for high temperature, high pressure hydrogen-hydrocarbon systems, *6th World Petroleum Congress*, Frankfurt am Main, Germany, 19–26 June, pp. 169–181.
- Hildebrand J.H. (1916) Solubility. *Journal of the American Society* **38**, 8, 1452–1473.
- Huang H.H., Lin H.M., Tsai F.N., Chao K.C. (1988) Solubility of Synthesis Gases in Heavy *n*-Paraffins and Fischer-Tropsch Wax, *Ind. Eng. Chem. Res.* **27**, 1, 162–169.
- Le Thi C., Tamouza S., Passarello J.P., Tobaly P., de Hemptinne, J.C. (2006) Modeling Phase Equilibrium of H_2 + *n*-Alkane and CO_2 + *n*-Alkane Binary Mixtures Using a Group Contribution Statistical Association Fluid Theory Equation of State (GC-SAFT-EOS) with a k_{ij} Group Contribution Method, *Ind. Eng. Chem. Res.* **45**, 20, 6803–6810.
- Lin H.M., Sebastian H.M., Chao K.C. (1980a) Gas-Liquid Equilibrium in Hydrogen + *n*-Hexadecane and Methane + *n*-Hexadecane at Elevated Temperatures and Pressure, *J. Chem. Eng. Data* **25**, 3, 252–254.
- Lin H.M., Sebastian H.M., Chao K.C. (1980b) Gas-Liquid Equilibria of Hydrogen + 1-Mehtyl Naphthalene at 457°C, *Fluid Phase Equilib.* **4**, 321.
- Lin H.M., Sebastian H.M., Simnick J.J., Chao K.C. (1981) Solubilities of Hydrogen and Methane in Coals Liquids, *Ind. Eng. Chem. Process Des. Dev.* **20**, 2, 253–256.
- Malone P.V., Kobayashi R. (1990) Ligth Gas Solubility in Phenanthrene: The Hydrogen-Phenanthrene and Methane-Phenanthrene, *Fluid Phase Equilib.* **55**, 193–205.
- Moysan J.M., Huron J.M., Paradowski H., Vidal J. (1983) Prediction of the solubility of hydrogen in hydrocarbon solvents through cubic equation of state, *Chem. Eng. Sci.* **38**, 7, 1085–1092.
- Park J., Robinson R.L., Gasem K.A.M. (1995) Solubilities of Hydrogen in Heavy Normal Paraffins at Temperatures from 323.2 to 423.2 K and Pressure to 17.4 MPa, *J. Chem. Eng. Data* **40**, 1, 241–244.
- Park J., Robinson R.L., Gasem K.A.M. (1996) Solubilities of Hydrogen in Aromatic Hydrocarbons from 323 to 433 K and Pressures to 21.7 MPa, *J. Chem. Eng. Data* **41**, 1, 70–73.
- Riazi M.R. (2005) *Charaterization and Properties of Petroleum Fractions*, ASTM International, Conshohocken, PA, 1st Edition.
- Riazi M.R., Al-Sahhaf T.A. (1996) Physical Properties of Heavy Petroleum Fractions and Crude Oils, *Fluid Phase Equilib.* **117**, 271–224.
- Riazi M.R., Vera J.H. (2005) Method to Calculate the Solubilities of Light Gases in Petroleum and Coal Liquid Fractions on the Basis of Their P/N/A Composition, *Ind. Eng. Chem. Res.* **44**, 1, 186–192.
- Riazi M.R., Roomi Y.A. (2007) A method to predict solubility of hydrogen in hydrocarbons and their mixtures, *Chem. Eng. Sci.* **62**, 6649–6658.

- Robinson R.L., Chao K.C. (1971) A Correlation of Vaporization Equilibrium Ratios for Gas Processing Systems, *Ind. Eng. Chem. Process Des. Dev.* **10**, 2, 221-229.
- Scatchard G. (1931) Equilibria in Non-Electrolyte Solutions in Relation to the Vapor Pressure and Densities of the Components, *Chemical Reviews* **8**, 2, 321-333.
- Scatchard G., Hildebrand J.H. (1934) Non-Electrolyte Solutions, *Journal of the American Society* **54**, 4, 995-996.
- Sebastian H.M., Simnick J.J., Lin H.M., Chao K.C. (1980) Gas-Liquid Equilibrium in the Hydrogen + *n*-Decane System at Elevated Temperatures and Pressures, *J. Chem. Eng. Data* **25**, 1, 68-70.
- Shaw J.M. (1987) A Correlation for Hydrogen Solubility in Alicyclic and Aromatic Solvents, *Can. J. Chem. Eng.* **65**, 293-298.
- Smith J.M., Van Ness H.C., Abbott M.M. (1996) *Introduction to Chemical Engineering Thermodynamics*, McGraw-Hill, New York, 5th Edition.
- Srinivas G., Field R., Watanasiri S., Herzog H. (2012) Correlation to predict solubility of hydrogen and carbon monoxide in heavy paraffins, *Fluid Phase Equilib.* **320**, 11-25.
- Tran T.K.S., NguyenHuynh D., Ferrando N., Passarello J.P., de Hemptinne J.C., Tobaly P. (2009) Modeling VLE of H₂ + Hydrocarbon Mixtures Using a Group Contribution SAFT with *k_{ij}* Correlation Method Based on London's Theory, *Energy Fuels* **23**, 2658-2665.
- Twu C.H., Coon J.E., Harvey A.H., Cunningham J.R. (1996) An Approach for the Application of a Cubic Equation of State to Hydrogen-Hydrocarbon Systems, *Ind. Eng. Chem. Res.* **35**, 3, 905-910.
- Walas M.W. (1985) *Phase Equilibria in Chemical Engineering*, Butterworth-Heinemann, Massachusetts.
- Yao J., Sebastian H.M., Lin H.M., Chao K.C. (1977-1978) Gas-Liquid Equilibria in Mixtures of Hydrogen and 1-Methyl Naphthalene, *Fluid Phase Equilib.* **1**, 4, 293-304.
- Zernov V.S., Kogan V.B., Egudina O.G., Kobayakov V.M., Babayants T.V., Kalichava L.I. (1990) Phase Equilibria and Volume Ratios in the Systems Heptane and Ethylene, *J. Appl. Chem. USSR* **63**, 7, 1469-1472.

*Final manuscript received in August 2012
Published online in April 2013*

Copyright © 2013 IFP Energies nouvelles

Permission to make digital or hard copies of part or all of this work for personal or classroom use is granted without fee provided that copies are not made or distributed for profit or commercial advantage and that copies bear this notice and the full citation on the first page. Copyrights for components of this work owned by others than IFP Energies nouvelles must be honored. Abstracting with credit is permitted. To copy otherwise, to republish, to post on servers, or to redistribute to lists, requires prior specific permission and/or a fee: Request permission from Information Mission, IFP Energies nouvelles, fax. +33 1 47 52 70 96, or revueogst@ifpen.fr.

APPENDIX A

A.1 Prediction of Critical Pressure and Critical Temperature

Simplified equations to calculate P_c and T_c of petroleum fractions in the range of C_5 - C_{20} are given by following equations (Riazi, 2005):

$$P_c = 3.1958 \times 10^5 [\exp(-8.505 \times 10^{-3} T_b - 4.8014 SG + 5.749 \times 10^{-3} T_b SG)] T_b^{-0.4844} SG^{4.0846} \quad (A.1)$$

$$T_c = 9.5233 [\exp(-9.314 \times 10^{-4} T_b - 0.544442 SG + 6.4791 \times 10^{-4} T_b SG)] T_b^{0.81067} SG^{0.53691} \quad (A.2)$$

where P_c is the critical pressure (bar); T_b is the normal boiling temperature (K); SG is the specific gravity at 15.5°C (obtained from density) and T_c is the critical temperature (K).

These equations are recommended only for hydrocarbons in the molecular weight range of 70-300. They were adopted by the API and have been used in many industrial computer softwares under the API method.

For heavy hydrocarbons ($>C_{20}$) the following equations are recommended (Riazi, 2005):

$$P_c = 6.9575 [\exp(-1.35 \times 10^{-2} T_b - 0.3129 SG + 9.174 \times 10^{-3} T_b SG)] T_b^{0.6791} SG^{-0.6807} \quad (A.3)$$

$$T_c = 35.9413 [\exp(-6.9 \times 10^{-4} T_b - 1.4442 SG + 4.91 \times 10^{-4} T_b SG)] T_b^{0.7293} SG^{1.2771} \quad (A.4)$$

A.2 Prediction of Acentric Factor

The acentric factor, ω , is a measure of the shape of the vapour pressure curve. Values of the acentric factor can be obtained using T_c , P_c and vapour pressure. Most recently Korsten (Riazi, 2005) modified the Clapeyron equation for vapour pressure of hydrocarbon systems and derived following equation:

$$\omega = 0.5899 \left(\frac{T_{br}^{1.3}}{1 - T_{br}^{1.3}} \right) \times \left[\log \left(\frac{P_c}{1.01325} \right) \right] - 1 \quad (A.5)$$

where ω is the acentric factor, T_{br} is the reduced normal boiling temperature (K) and P_c is the critical pressure (bar).

A.3 Prediction of Molar Volume

Molar volume at 25°C is calculated from density at the same temperature and molecular weight. If density is given at another temperature, following equation may be used to obtain density at any temperature once a value of density is known (Riazi, 2005):

$$\frac{(\rho_T - \rho_0)}{(T - T_0)} = -10^{-3} \times (2.34 - 1.9\rho_T) \quad (A.6)$$

where ρ_0 is the density (g/cm^3) at T_0 (for example 298.15 K) and ρ_T is the density (g/cm^3) at given temperature T .

A.4 Prediction of Solubility Parameter

Three methods to calculate the solubility parameter are considered as is shown in Table 11. They are described in the text.